Stable Kinematic Teleoperation of Wheeled Mobile Robots with Slippage using Time-Domain Passivity Control

Weihua Li[a,b], Zhen Liu[a,*], Haibo Gao[a], Xuefeng Zhang[c] and Mahdi Tavakoli[b,†]

[a] *State Key Laboratory of Robotics and System, Harbin Institute of Technology, Harbin 150001, China*
[b] *Department of Electrical & Computer Engineering, University of Alberta, Edmonton, Alberta T6G 2V4, Canada*
[c] *Beijing Institute of Astronautical Systems Engineering, Beijing 100076, China*

Abstract—**Wheel slippage creates control challenges for wheeled mobile robots (WMR). This paper proposes a new method for haptic teleoperation control of a WMR with longitudinal slippage by using the time-domain passivity control (TDPC) approach. We show the potential nonpassivity for the environment termination caused by the slippage dynamics. The utilized TDPC approach maintains the passivity of teleoperation system terminations through a passivity observer and a passivity controller at the environment termination. The teleoperation controllers are then simply constrained by Llewellyn's absolute stability criterion for closed-loop stability purposes. Experiments with the proposed controller demonstrate that it can result in stable bilateral teleoperation with a satisfactory tracking performance with TDPC.**

Index Terms—**Wheeled mobile robot, kinematics, longitudinal slippage, teleoperation, absolute stability.**

Nomenclature

r	Wheel's radius
v_s, v_{sd}	Wheel's linear velocity and desired linear velocity
ω_s, ω_{sd}	Wheel's angular velocity and desired angular velocity
S	Wheel's slippage
q_m	Master robot's position
M_m, B_m	Master robot's mass and damping
Z_m, Z_s	Impedances of master and slave robots
Z_h, Z_e	Impedances of human and environment
τ_h, δ_e	Human and environment interaction forces
PC	Passivity controller
PO	Passivity observer
HT	Human termination
ET	Environment termination

* Corresponding author. Tel.: +86 0451 86402037.

† Corresponding author. Tel.: +1 780 4928935.

E-mail address: {liweihua.08301, liuzhen_hit}@163.com (W. Li, Z. Liu), gaohaibo@hit.edu.cn (H. Gao), xfzhangmail@126.com (X. Zhang), mahdi.tavakoli@ualberta.ca (M. Tavakoli (Principal Investigator)).

1. Introduction

When a wheeled mobile robot (WMR) is travelling on a slippery or soft surface, the ideal assumption of pure rolling of wheels does not hold. The introduction of wheel slippage affects the WMR's kinematic and dynamic models, creating challenges for control. The increasing interest in planetary exploration using WMRs has attracted more attention to the slippage phenomenon, which causes a velocity loss for the WMR relative to a desired input velocity [1-5]. To compensate for the influence of the wheel's slippage on WMR's velocity, a path planning method is proposed in [4]. A control algorithm is proposed in [5] where the forces between the WMR and the terrain are modeled based on the value of slippage, but this slippage-dependent interaction force model is always experimental and its fidelity is limited by the uncertainty in determining its parameters [1-2].

WMR teleoperation is beneficial when using the robot in outer space, and appropriately providing haptic feedback to the operator (i.e., bilateral teleoperation) can enhance the operator's navigation and control capability [6]. Different from a holonomic constrained robot's teleoperation [7], the bilateral teleoperation of a WMR involves two kinematics-related challenges that are often not experienced during teleoperation of non-mobile robots [8]: 1) The workspace of the master robot is limited, but that of the slave mobile robot is unlimited or much bigger, and 2) the wheeled mobile robot is under non-holonomic constraints so the directions of permissible motions are restricted; this is topic of study in the literature [12]. Owing to WMR's unlimited workspace, coordination of the master's position with the slave's velocity has commonly been a goal of WMR teleoperation [8-13].

In this paper, for the first time we consider simultaneously the problem of *workspace mismatch* and *surface slippage* for a two-wheeled actuated mobile robot that travels forward/ backward but does not rotate and, therefore, is free from non-holonomic constraints. We show that using kinematic control for a WMR experiencing longitudinal slippage, there is a shortage of passivity (SOP) [14] caused by the slippage dynamics in a termination of the teleoperation system[‡] (the other termination is the human operator dynamics augmented with the position/velocity transformation). We will use time-domain passivity control (TDPC) to maintain the teleoperation system termination's passivity through a passivity observer (PO) and a passivity controller (PC) at that terminal. Then, the teleoperator dynamics are subjected to Llewellyn's absolute stability criterion, which assumes the passivity of both terminations, in order to find conditions on the controller gains.

In non-mobile robot contexts, TDPC is used in [15] to compensate for the nonpassivity caused by the controllers of a teleoperation system, having assumed the passivity of the terminations. In [16], to deal with the shortage of passivity of one or both of terminations in a regular teleoperation system, an absolute stability criterion is proposed, which requires the magnitude of the SOP to be known. These have not been done in the context of position/rate control suitable for WMR teleoperation.

In this paper, after addressing the problem of termination nonpassivity that results from the slippage dynamics through TDPC, Llewellyn's absolute criterion is used to design the WMR teleoperation system's controller.

[‡] A WMR's embedded controller is typically at the kinematic level and useful for wheel angular velocity control rather than at the dynamic level and useful for wheel torque control.

The rest of this paper is organized as follows. In Sec. II, the WMR teleoperation system is introduced, and the nonpassivity existing in the environment (i.e., the slippage between the WMR and the terrain) termination (ET) is analyzed. In Sec. III, the PO/PC is used to compensate for the termination's nonpassivity, and the WMR teleoperation system controller is designed using Llewellyn's absolute stability criterion. In Sec. IV, in order to demonstrate the system stability, experiments of the proposed methods are conducted using a Phantom Premium 1.5A robot (Geomagic Inc., Wilmington, MA, USA) as the master and the ROSTDyn (Rover Simulation based on Terramechanics and Dynamics) WMR simulation platform as the slave [17]. Sec. V presents the concluding remarks and future work.

2. Teleoperation of a WMR with longitudinal slippage

As mentioned before, owing to the unlimited workspace of the WMR, the coordination of the position of the master robot with the velocity of the slave is needed. We will also feed back certain information characterizing the interaction between the slave WMR robot and the terrain as a force to the human operator.

2.1. Slave robot's model

When the WMR is traveling on a soft terrain (e.g., loose soil or sand), due to the limited friction force generated by the terrain and possible opposing external forces such as that coming from hitting an obstacle, the wheel's linear velocity v_s will not be equal to the wheel's angular velocity ω times the wheel's radius r. Slippage S can be defined as [5]

$$S = \begin{cases} (r\omega_s - v_s)/v_s & (\omega_s \neq 0) \\ 0 & (\omega_s = 0) \end{cases} \tag{1}$$

In order to compensate for the velocity loss caused by the slippage, an acceleration-level controller for the motor is used in this paper as Fig. 1 shows. In Fig. 1, we assume that the transfer function from $\dot{\omega}_{sd}$ to $\dot{\omega}_s$ is unity. By differentiating $Sv_s = r\omega_s - v_s$ obtained from (1), we can get the WMR model relating the wheel's angular acceleration $\dot{\omega}_s$ to its linear acceleration $\dot{v}_s$ as

$$r\left(\dot{\omega}_s - \underbrace{\frac{1}{r}\left(S\dot{v}_s + \dot{S}v_s \right)}_{slippage\ model} \right) = \dot{v}_s, \tag{2}$$

where the slippage model enters the relationship between the WMR's angular acceleration and linear acceleration.
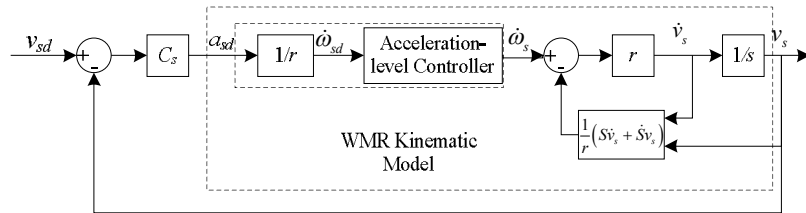

Fig. 1. Simplified WMR's kinematic model.

Based on the controller for the WMR in Fig. 1, the WMR and the ET can be modeled as Fig. 2

shows. Here, f_s is the force feedback sent from the slave WMR robot to the master robot. By defining the control input $u_s = a_{sd} = r\dot{\omega}_{sd}$ (desired acceleration for the slave robot) and the environment interaction force δ_e (including the slippage phenomenon and any other force the environment applies to the slave robot such as when hitting an obstacle) as

$$\delta_e(t) = S(t)\dot{v}_s(t) + \dot{S}(t)v_s(t). \tag{3}$$

the kinematic model of the slave robot can be found from (2) as

$$\dot{v}_s = u_s - \delta_e, \tag{4}$$

The above provides a straightforward model of the WMR as the slave robot in interaction with an environment.
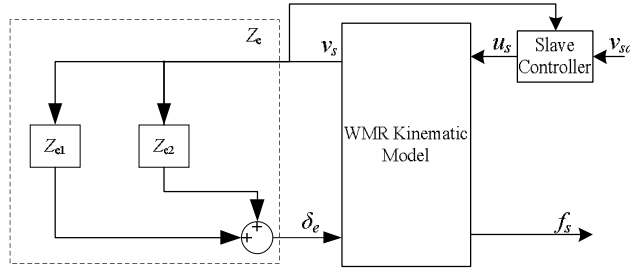
Fig. 2. Model of slave robot & ET in WMR's bilateral teleoperation (f_s is feedback to master robot).

Based on the definition of passivity in [18], having the input $v_s(t)$ and the output $\delta_e(t)$, the ET (3) satisfies the following inequality for all $v_s(t)$ and $T \geq 0$:

$$\int_0^T \delta_e(t)v_s(t)dt = \int_0^T v_s(t)\left(S(t)\dot{v}_s(t) + \dot{S}(t)v_s(t)\right)dt$$
$$= \underbrace{V(T) - V(0)}_{Z_{e1}} + \underbrace{\frac{1}{2}\int_0^T \dot{S}(t)v_s(t)v_s(t)dt}_{Z_{e2}}, \tag{5}$$

where $V(t) = \frac{1}{2}S(t)v_s^2(t)$.

As shown above, the ET is decomposed into two components (Fig. 2): One is Z_{e1}, which may cause nonpassivity when $S(t)$ is negative (WMR is sliding) (if $S(t)$ is positive, Z_{e1} is passive), and the other is Z_{e2}, which may also cause nonpassivity when $\dot{S}(t)$ is negative. *Specially, if S(t) is positive with a negative $\dot{S}(t)$, the decreasing slippage will increase the slave WMR's velocity, which means the environment generates unexpected energy.* Therefore, the system (3) is in risk of nonpassivity.

2.2. Master robot's model

For a single-joint master robot, the dynamics can be written as

$$M_m\ddot{q}_m + B_m\dot{q}_m = \tau_m + \tau_h, \tag{6}$$

where M_m and B_m are the robot's mass and damping, q_m is the joint angle, and τ_m and τ_h are the forces/torques applied by the master robot controller and the human, respectively.

Due to the unlimited workspace of the WMR, in order to solve the coordination between the master's position q_m and the slave's velocity v_s, a new variable $r_m = \lambda\dot{q}_m + q_m$ where $0 < \lambda < 1$ is used (instead of either q_m or $\dot{q}_m$) in the impedance matrix [8]. This change of variable also requires the

definition of a new control signal. The controller τ_m in (6) is designed as $\tau_m = \tau_m^* + \bar{\tau}_m$ consisting of a local controller τ_m^* and $\bar{\tau}_m$ that will be designed in Sec. III. In terms of the new variable r_m and with the local controller $\tau_m^* = -B_{Lv}\dot{q}_m - B_{Lp}q_m$, the master robot's dynamic model (6) can be rewritten as

$$\bar{M}_m \dot{r}_m + \bar{B}_m r_m = \bar{\tau}_m + \tau_h, \tag{7}$$

where $\bar{M}_m = M_m/\lambda$, $\bar{B}_m = B_{Lp}$ and $B_{Lv} = \dfrac{M_m}{\lambda} + \lambda B_{Lp} - B_m$.

As [8] presented, we assume the human operator can adjust his/her impedance to ensure the passivity of its impedance when augmented with the position/velocity transformation.

3. Main Results

Following the above-described master and slave robot's model, the WMR teleoperation system can be modeled as the two-port network in Fig. 3. Assume that for the teleoperation system with the master robot (7) and the slave robot (4), the impedance matrix model for the two-port network in Fig. 3 is

$$\begin{bmatrix} \tau_h \\ \delta_e \end{bmatrix} = \begin{bmatrix} Z_{11} & Z_{12} \\ Z_{21} & Z_{22} \end{bmatrix} \begin{bmatrix} r_m \\ -v_s \end{bmatrix}, \tag{8}$$

In general, the Llewellyn's criterion can be employed to ensure the stability of a two-port network with passive terminations.
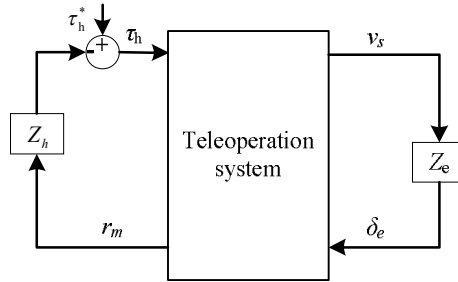

Fig. 3. WMR's bilateral teleoperation system.

Lemma 1 (Llewellyn's criterion [19]) The two-port network (8) is absolutely stable (i.e., the overall system in Fig. 3 is bounded-input/bounded output stable assuming the passivity of both terminations) if and only if

(1) $Z_{11}(s)$ and $Z_{22}(s)$ have no poles in the right half plane;

(2) Any poles of $Z_{11}(s)$ and $Z_{22}(s)$ on the imaginary axis are simple with real and positive residues;

(3) For $s = j\omega$ and all real values of ω:

$$\begin{array}{l} \mathrm{Re}(Z_{11}) \geq 0 \\ \mathrm{Re}(Z_{22}) \geq 0 \\ 2\,\mathrm{Re}(Z_{11})\,\mathrm{Re}(Z_{22}) - \mathrm{Re}(Z_{12}Z_{21}) - \left| Z_{12}Z_{21} \right| \geq 0 \end{array} \tag{9}$$

In practice, however, since the ET may show a nonpassive behavior owing to the slippage and other external forces, the Llewellyn's absolute stability criterion (9) is not sufficient for the teleoperation

system stability analysis. Therefore, a time-domain passivity controller (PC_e) is used for the ET in order to make it passive. This local controller alters the output of the ET such that

$$\underbrace{\begin{bmatrix} \tau_h \\ \delta_e \end{bmatrix} + \begin{bmatrix} 0 \\ PC_e \end{bmatrix}}_{\text{New Modified Terminations}} = \begin{bmatrix} Z_{11} & Z_{12} \\ Z_{21} & Z_{22} \end{bmatrix} \begin{bmatrix} r_m \\ -v_s \end{bmatrix}. \tag{10}$$

3.1. TDPC for bilateral teleoperation of a WMR

In [15], a passivity controller (PC) is proposed to compensate for a 2-port network's nonpassive energy, which can be detected by a passivity observer (PO). In this paper, we do not apply TDPC on the 2-port network. Instead, TDPC is employed to locally compensate for the nonpassivity of the ET as Fig. 4 shows. Accordingly, the utilized passivity observers monitor for the nonpassivity of this termination (and not that of the 2-port network).
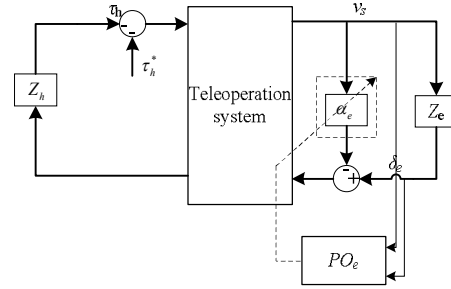
Fig. 4. WMR's teleoperation scheme with TDPC control.

The PC is essentially a variable damper α_e that dissipates energy and is designed through the following process, which describes how to tune α_e.

1) Assuming that the slave robot's velocity v_s and the ET's output force δ_e are constant during each sampling period, the PO for the ET observes the sum of the energy generated by the ET from 0 to n and the energy generated by the PC from 0 to n-1. Thus,

$$E_e(n) = E_e(n-1) + \left(\delta_e(n)v_s(n) + \alpha_e(n-1)v_s^2(n-1)\right)\Delta T . \tag{11}$$

2) When the PO output is negative, which indicates that the termination is nonpassive at time n (assuming the initial energy at $t = 0$ was zero), the PC compensates for the nonpassive energy through a damping; otherwise the damping is zero:

$$\alpha_e(n) = \begin{cases} -\dfrac{E_e(n)}{v_s^2(n)\Delta T} & \text{if } E_e(n) < 0 \\ 0 & \text{if } E_e(n) \geq 0 \end{cases}. \tag{12}$$

3) The passivity controller is activated, effectively changing the input to the slave robot as

$$u_s^* = u_s + \alpha_e(n)v_s(n), \tag{13}$$

With the PC in (13), it is easy to prove that the modified ET is passive:

$$\begin{aligned} \tilde{E}_e(n) &= E_e(n) + \alpha_e(n)v_s^2(n)\Delta T \\ &\geq E_e(n) - \dfrac{E_e(n)}{v_s^2(n)\Delta T}v_s^2(n)\Delta T \\ &\geq 0 \end{aligned} \tag{14}$$

Once the ET is controlled to be passive, we can design the WMR's bilateral teleoperation system with the Llewellyn's criterion.

3.2. Teleoperation system design

After using the TDPC to compensate for the potentially nonpassive ET, Lemma 1 is utilized to design the WMR's bilateral teleoperation system. The PEB (position error based) and DFR (direct force reflection) teleoperation architectures are considered in this paper [20]. Fig. 5 and Fig. 6 show these two teleoperation architectures encompassing the PC and PO used at the ET. The PC is a local controller and part of the ET's dynamics.
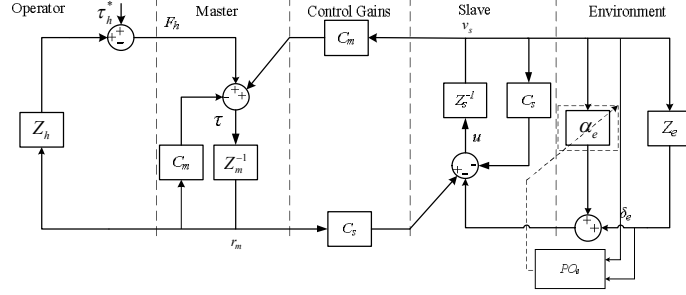
Fig. 5. PEB teleoperation control of a WMR.
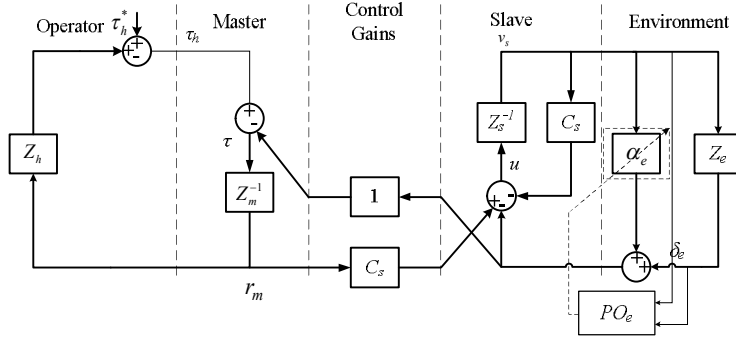
Fig. 6. DFR teleoperation control of a WMR.

The impedance matrix of the bilateral teleoperation system (8) was modified to (10) in the presence of a PC for the ET. This impedance matrix can be rewritten as

$$\begin{bmatrix} \tau_h \\ \delta_e + \alpha_e v_s \end{bmatrix} = \begin{bmatrix} Z_{11} & Z_{12} \\ Z_{21} & Z_{22} \end{bmatrix} \begin{bmatrix} r_m \\ -v_s \end{bmatrix}. \tag{15}$$

We showed in (14) that the ET when combined with its respective PC is passive. Therefore, in order to design a stable bilateral teleoperation system, it suffices to focus on the right-hand side of (15). As far as transparency, in the DFR architecture, the output of the PC for the ET is added to δ_e, thus the force feedback is inevitably perturbed to some extent.

For the PEB architecture in Fig. 5, the impedance matrix $\mathbf{Z}$ in (15) is

$$Z = \begin{bmatrix} \bar{M}_m s + \bar{B}_m + C_m & C_m \\ C_s & s + C_s \end{bmatrix}.$$

According to Lemma 1, the following conditions should be met for stability of the PEB teleoperation system (details of derivations not shown for brevity):

$$\overline{B}_m + C_s \geq 0$$
$$C_s \geq 0 \qquad .$$
$$\overline{B}_m \geq 0$$
(16)

To design the DFR control architecture in Fig. 6, the impedance matrix Z in (15) is

$$Z = \begin{bmatrix} \overline{M}_m s + \overline{B}_m + C_s & s + C_s \\ C_s & s + C_s \end{bmatrix}.$$

According to Lemma 1, the following conditions should be met for stability of the DFR teleoperation system:

$$\overline{B}_m + C_s \geq 0$$
$$C_s \geq 0 \qquad .$$
$$\overline{B}_m \geq 0 \ \left(C_s >> \omega \right)$$
(17)

In the stability conditions of (16) and (17), there is no trace of the environment termination's nonpassivity as it was compensated for via TDPC locally.

4. Experimental results and discussion

In the case studies below, we consider the teleoperation of a mobile robot in an environment with slippage. As the slippage varies with soil's mechanical parameters (e.g., friction angle) [21] and the terrain's parameters (e.g., slope angle), a PC will be used to compensate for the nonpassivity in real-time so that the slave robot's environment remains passive.

Limited by practical challenges related to recreating specific terrain characteristics that give rise to certain shortage of passivity of the environment model, we perform semi-physical experiments to validate the proposed DFR and PEB teleoperation of the WMR under longitudinal slippage.

4.1. Experimental setup

To validate the proposed methods, experiments are done using the Phantom Premium 1.5A haptic device (master robot) and ROSTDyn (slave robot). The experimental system is detailed below.

(1) Master robot and human operator

As shown in Fig. 7, in our WMR's bilateral teleoperation system, the master robot is a Phantom Premium 1.5A haptic device (Geomagic Inc., Wilmington, MA, USA) (Fig. 7), and the slave robot (WMR) is a WMR's simulation platform called ROSTDyn which has been developed by the authors [17], and the communication between the master robot and the slave robot is implemented using local area network (LAN). Considering just one degree of freedom (DOF) motion, the first joint q_1 of the Phantom is used and the other two joints are locked by a high gain position controller ($q_2 = q_3 = 0$) (Fig. 8). Based on the research results from [22], the Phantom's inertia is $M_m = 0.0035$. In (7), $\lambda = 0.1$ and $B_{Lv} = -0.035$.
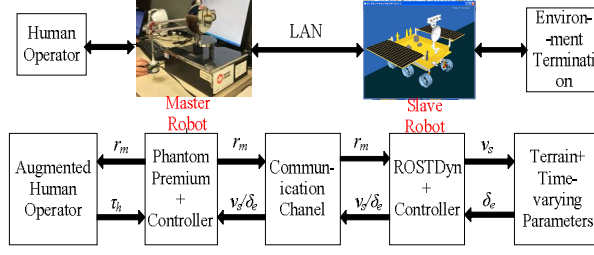
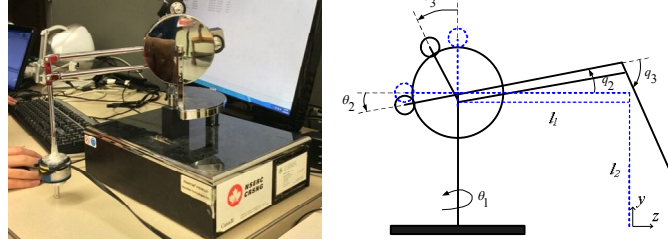Fig. 7. Scheme of WMR bilateral teleoperation system.

Fig. 8. Structure sketch of master robot.

In the following experiments, based on (7), the force applied on the master robot is estimated as

$$\tau_h = \bar{M}_m \dot{r}_m + \bar{B}_m r_m - \bar{\tau}_m . \tag{18}$$

(2) Slave robot and environment

As shown in Fig. 7, ROSTDyn is used as the slave robot and developed based on Vortex software (CMLabs, Montreal, Canada) and the simplified terramechanics model. ROSTDyn can realize a real-time simulation with a good fidelity [17]. In this paper, we use ROSTDyn to simulate a WMR moving on a soft terrain, which causes slippage. The slippage is time-varying with the changing terrain. The terramechanics model between the wheel and terrain in ROSTDyn is the following:

$$\begin{cases} F_N = rb\sigma_m A + rb\tau_m B = AX + BY \\ F_{DP} = rb\tau_m A - rb\sigma_m B = AY - BX , \\ M_R = r^2 b(\theta_1 - \theta_2)\tau_m/2 = rCY \end{cases} \tag{19}$$

where $A = \dfrac{\cos\theta_m - \cos\theta_2}{\theta_m - \theta_2} + \dfrac{\cos\theta_m - \cos\theta_1}{\theta_1 - \theta_m}$;

$B = \dfrac{\sin\theta_m - \sin\theta_2}{\theta_m - \theta_2} + \dfrac{\sin\theta_m - \sin\theta_1}{\theta_1 - \theta_m}$; $C = (\theta_1 - \theta_2)/2$;

$X = rb\sigma_m$; $Y = rb\tau_m$;

$\tau_m = E(c + \sigma_m \tan\varphi)$; $\sigma_m = K_s r^N (\cos\theta_m - \cos\theta_1)^N$;

$E = 1 - \exp\{-r[(\theta_1 - \theta_m) - (1-s)(\sin\theta_1 - \sin\theta_m)]/K\}$; $K_S = K_c/b + K_\varphi$; $N = n_0 + n_1 s$.

In (19), F_N is the normal force, F_{DP} is the drawbar pull force, and M_R is the moment generated by the interaction between the wheel and the terrain; s is the slippage of a wheel and φ is the internal friction angle; and the other parameters are introduced in [23].

The terrain has a slope with an angle of 15°, and the terrain size is 10m (x)×10m (y). Since in this paper, we are focusing on creating a nonpassive ET caused by the slippage, and the slippage model cannot be directly given, the most sensitive parameter to the slippage [24], which is φ in (19), is considered and set as a terrain-varying function. For a real terrain, the parameter φ in (19)

is one of the soil's intrinsic mechanical characteristics. The following model makes the terrain become harder as the WMR travels forward:

$$\varphi = \begin{cases} 0.7 + 0.1(x - 2.1) & (2.1 \le x < 9.0) \\ 0.7 & (0 < x < 2.1) \end{cases}, \qquad (20)$$

Here, x is the WMR position along the moving direction. In the case of climbing a sloped terrain, the bigger the φ, the smaller the slippage, which will cause a negative $\dot{S}$ while S is positive, which causes the ET's potential nonpassivity.

In the experiments, the PC for the ET is designed based on Sec. III, and is embedded into the slave controller. The teleoperation controllers for PEB and DFR are designed based on conditions (16) and (17). The frequency for the PO is set at 30 Hz. The maximum value of the PC damper is set at 3.0.

4.2. PEB Experiments

In the experiments involving WMR bilateral teleoperation with PEB architecture, based on (16), the teleoperator parameters are set to be $C_m = 10$, $C_s = 20$, $\bar{B}_m = 0$. Then, the stability conditions (16) obtained from the Llewellyn's criterion is satisfied for the right-hand side of (15) in all cases reported below. To validate the proposed methods, the experiments with/without PCs are done under the same teleoperator parameters, and the experimental results are shown in Fig. 9 (without TDPC) and Fig. 10 (with TDPC).

For the PEB architecture, the master robot provides r_m, which acts as a reference value for to the slave robot's velocity. Owing to the time-varying slippage, the actual slave robot's velocity v_s may be different from this commanded velocity and a velocity-error is caused, which is fed back to the master robot as a force. If r_m is bigger than v_s, the human operator will feel a backward force that pushes back on the master robot; if r_m is smaller than v_s, the human operator will feel a forward force that pulls the master robot forward. Therefore, in PEB teleoperation, force feedback guides the human operator to give a more effective command to the slave WMR.

The position-velocity plots of the experiments without the TDPC (Fig. 9(a)) show that the PEB system with nonpassive ET is unstable. The ET's nonpassivity (Fig. 9(b)) will inject energy to the slave robot and make the actual velocity v_s diverge away from the commanded velocity r_m. As a result, the position-velocity coordination is not maintained and the human operator cannot control the slave WMR with this type of force feedback (Fig. 9(c)). In this experiment, owing to the big oscillation of the master robot's position, the coordination between q_m and v_s is poor as $\dot{q}_m$ is big (Fig. 9(a)).

Using TDPC, on the other hand, the termination's nonpassivity (Fig. 10(c)) is completely compensated for by the PC (Fig. 10(b)), resulting in a stable system (Fig. 10(a)). The position-velocity coordination is maintained well and it is easy for the human operator (Fig. 10(d)) to control the slave robot's velocity at a given level. One present drawback is poor force tracking performance (Fig. 10(d)), which is always expected from PEB teleoperation.
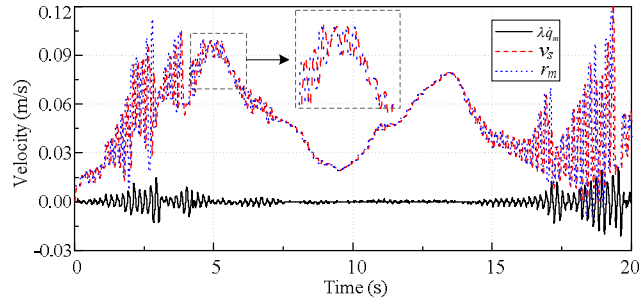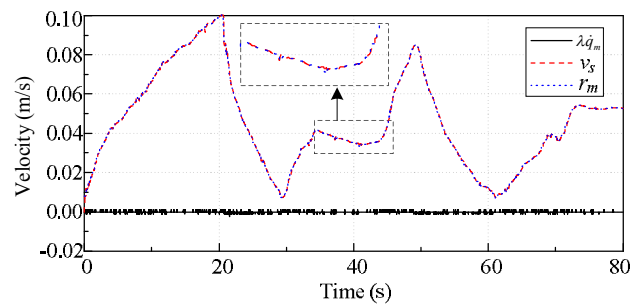
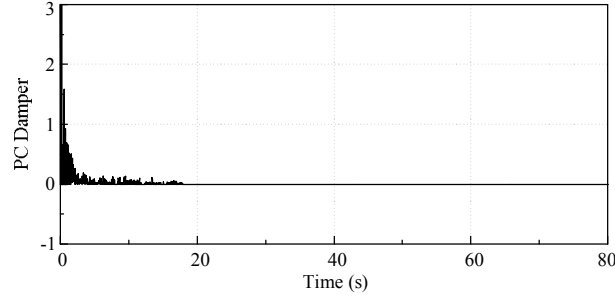(a) Position-velocity coordination.
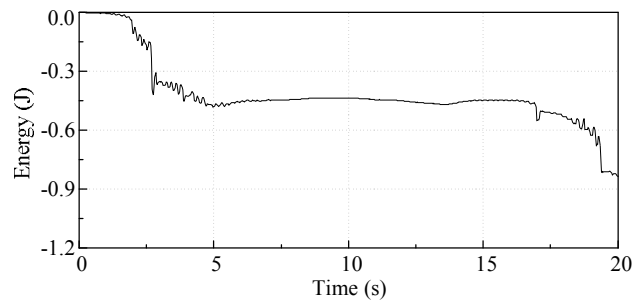
(b) Generated energy by ET
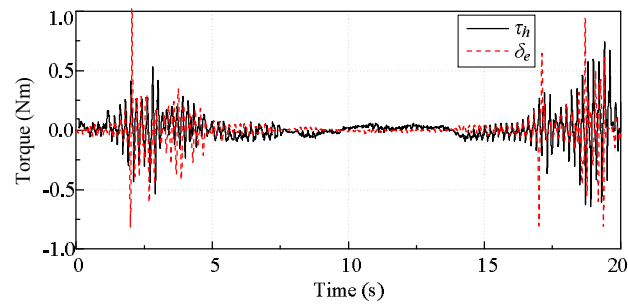
(c) Force tracking performance (τ_h and δ_e).
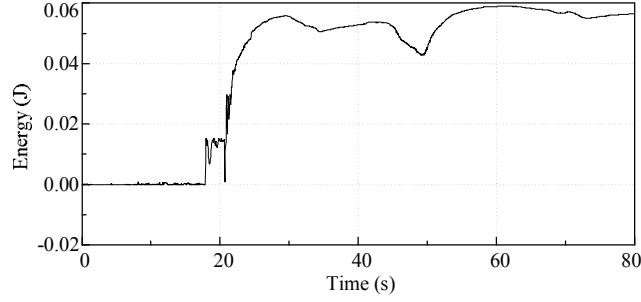
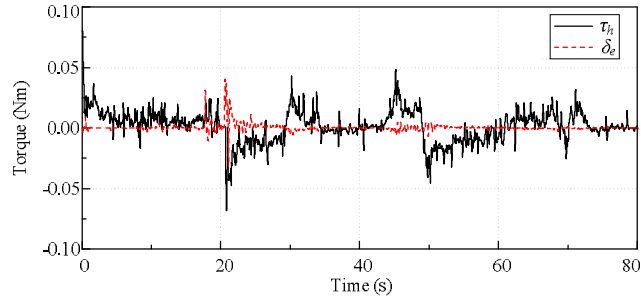Fig. 9. Experimental results for PEB without TDPC.

(a) Position-velocity coordination.

(b) PC damper.

(c) Generated energy by ET & PC.

(d) Force tracking performance (τ_h and δ_e).

Fig. 10. Experimental results for PEB with TDPC.

4.3. DFR Experiments

In the experiments of the WMR teleoperation with DFR architecture, based on (17), the teleoperator parameters are set as $C_s = 30$, $\bar{B}_m = 0$. Then, the stability conditions (17) obtained from the Llewellyn's criterion is satisfied for the right-hand side of (15) in all cases reported below.

Experiments with/without PCs are done under the same teleoperator parameters, and the experiment results are shown in Fig. 11 (without TDPC) and Fig. 12 (with TDPC). Note that here the force feedback is not the actual environment force, but is the actual environment force plus the force generated by the PC of the ET. The terrain parameters and φ are same as in the case of PEB.

In the DFR architecture, similar to PEB, the master robot provides r_m, which acts as a reference value for to the slave robot's velocity. Unlike PEB which fed back the *velocity error* as a force to the human operator, in DFR the ET's force δ_e is fed back to the human operator, which can be seen as an *acceleration error* based on (4). Physically speaking, if δ_e is positive, which means that the actual acceleration of the slave robot is smaller than the commanded acceleration, a backward force will be felt by the human operator informing the user about this deficiency in the WMR's

acceleration. If δ_e is negative, which means that the actual acceleration of the slave robot is bigger than the commanded acceleration, a forward force will be felt by the human operator to signal an excess in the WMR's acceleration. In both the PEB and the DFR force feedback schemes, the human operator receives useful feedback from the environment of the slave robot that should pave the ground for a more effective command; one feedback is about velocity error and the other is about acceleration error.

From the position-velocity plots of the experiments without the TDPC (Fig. 11(a)), it can be seen that the DFR system with a nonpassive ET is unstable (Fig. 11(a)). Specifically, the ET's nonpassivity (Fig. 11(b)) will inject additional energy to the master robot (note that δ_e is fed back to the master robot). As a result, the human operator (Fig. 11(c)) cannot effectively control the master robot's position at a constant value. In this experiment, owing to the big oscillation of the master robot's position, the coordination between q_m and v_s is poor as $\dot{q}_m$ is big (Fig. 11(a)).

Using TDPC, the terminations nonpassivity (Fig. 12(c)) is completely compensated for by the PC (Fig. 12(b)) and the system is stable (Fig. 12(a)). Specifically, with the PC, the position-velocity coordination is performed well and the human operator (Fig. 12(d)) can easily control the slave robot's velocity at a desired level. The tiny fluctuation after 20s in Fig. 12 may be induced by the human operator hand's shaking on a small scale during the experiments. Since the damping of the master robot is quite small, the human operator hand's shaking can easily affect its position, which can be addressed by decreasing the coefficient λ.
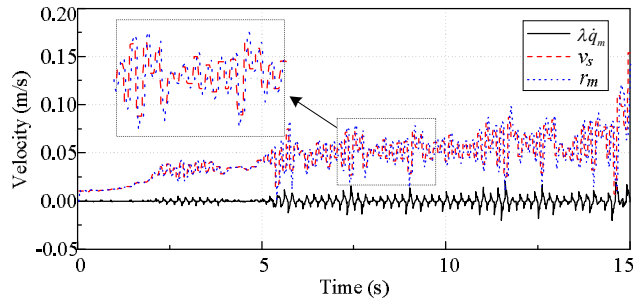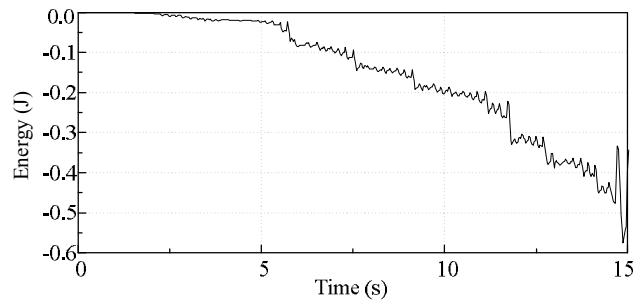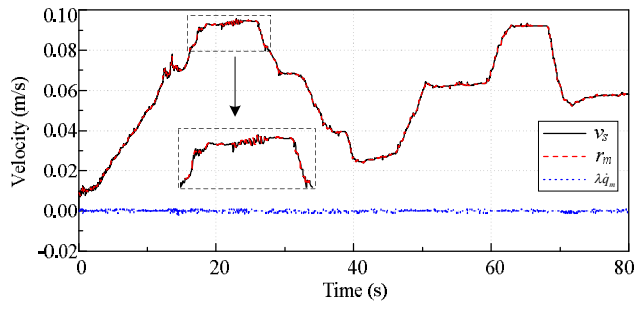

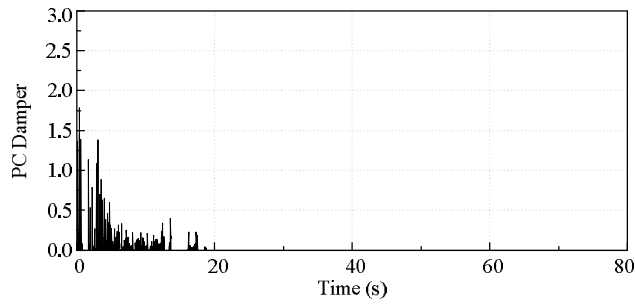(a) Position-velocity coordination.
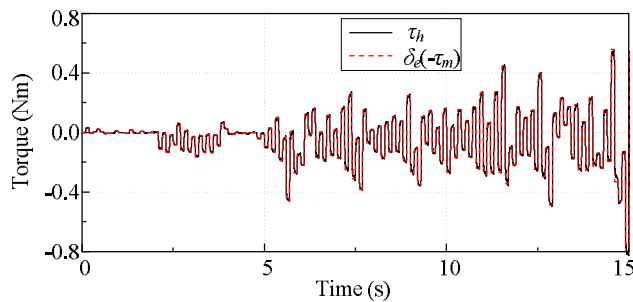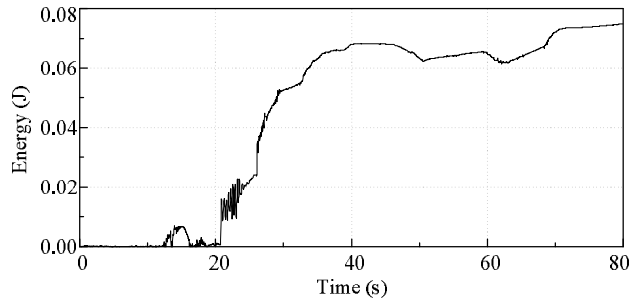

(b) Generated energy by ET.

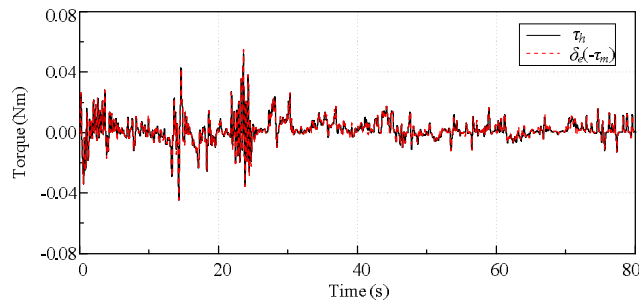Fig. 11. Experimental results for DFR without TDPC.

(a) Position-velocity coordination.

(b) PC damper.

(c) Generated energy by ET&PC.

(d) Force tracking performance (τ_h and δ_e).

Fig. 12. Experimental results for DFR with TDPC.

In summary, from the experimental results, it is concluded that the proposed method can effectively lead to a stable teleoperation system using TDPC to compensate for the termination's nonpassivity and the Llewellyn's criterion to stabilize the WMR's bilateral teleoperation system.

5. Conclusion

This paper presents a new method for haptic teleoperation control of a WMR with a nonpassive termination. Through the proposed TDPC approach, the environment termination, which can be made non-passive by the fluctuation of the slippage, is compensated for to be a passive system. With the proposed controllers, the WMR's velocity can track the master robot's position. The absolute stability conditions, which are acquired by the Llewellyn's criterion considering the passive environment termination after the compensation, lead to a stable teleoperation system with a good position-velocity coordination and a good force tracking performance.

In the future, the WMR's rotation motion and teleoperation time delays will be considered in the stability analysis and control design.

Acknowledgment

Reference

[1] L. Ding, H. Gao, Z. Deng, K. Yoshida, and K. Nagatani. Experimental study and analysis on driving wheels' performance for planetary exploration rovers moving in deformable soil. J. Terramech, 2011; 48 (1): 27–45.

[2] L. Ding, K. Nagatani, K. Sato, et al.. Terramechanics-based high-fidelity dynamics simulation for wheeled mobile robot on deformable rough terrain. In: Proceedings of the 2010 International Conference Robotics and Automation, Anchorage, Alaska, USA, 2010. p. 4922–4927.

[3] Giulio Reina, Lauro Ojeda, Annalisa Milella, and Johann Borenstein. Wheel Slippage and Sinkage Detection for Planetary Rovers. IEEE Transactions on Robotics, 2006; 11(2): 185-195.

[4] G. Ishigami, K. Nagatani, and K. Yoshida. Path Following Control with Slip Compensation on Loose Soil for Exploration Rover. In: Proceedings of the 2006 IEEE/RSJ International Conference on Intelligent Robots and Systems, Beijing, 2006. p. 5552-5557.

[5] Yu Tian and Nilanjan Sarkar. Control of a Mobile Robot Subject to Wheel Slip. J. Intell. Robot Syst., 2014; 74 (4): 915-929.

[6] Carolina Passenberg, Angelika Peer, Martin Buss. A survey of environment-, operator-, and task-adapted controllers for teleoperation systems. Mechatronics, 2010; 20 (7): 787-801.

[7] Zhijun Li, Xiaoqing Cao, Yong Tang, Rui Li, and Wenjun Ye. Bilateral Teleoperation of Holonomic Constrained Robotic Systems with Time-Varying Delays. IEEE Trans. Instrum. Meas., 2013; 62 (4): 752-765.

[8] Dongjun Lee, Oscar Martinez-Palafox, and Mark W. Spong. Bilateral Teleoperation of a Wheeled Mobile Robot over Delayed Communication Network. In: Proceedings of the 2006 IEEE International Conference on Robotics and Automation, Orlando, 2006. p. 3298-3303.

[9] Ildar Farkhatdinov and Jee-Hwan Ryu. Improving Mobile Robot Bilateral Teleoperation by Introducing Variable Force Feedback Gain. In: Proceedings of the 2010 IEEE/RSJ International Conference on Intelligent Robots and Systems, Taipei, 2010. p. 5812-5817.

[10] Farrokh Janabi-Sharifi and Iraj Hassanzadeh. Experimental Analysis of Mobile-Robot Teleoperation via Shared Impedance Control. IEEE Trans. Syst. Man Cybern. - Part B, 2011; 41 (2): 591-606.

[11] Ha Van Quang, Ildar Farkhatdinov and Jee-Hwan Ryu. Passivity of Delayed Bilateral Teleoperation of Mobile Robots with Ambiguous Causalities: Time Domain Passivity Approach. In: Proceedings of the 2012 IEEE/RSJ International Conference on Intelligent Robots and Systems, 2012. p. 2635-2640.

[12] Pawel Malysz and Shahin Sirouspour. A Task-space Weighting Matrix Approach to Semi-autonomous Teleoperation Control. In: Proceedings of the 2011 IEEE/RSJ International Conference on Intelligent Robots and Systems, San Francisco, 2011. p. 645-652.

[13] Ricardo Carelli, Guillermo Forte, Luis Canali, Vicente Mut, et. al. Autonomous and teleoperation control of a mobile robot. Mechatronics, 2008; 18 (4): 187-194.

[14] Beatriz Morales, Flavio Roberti, Juan Marcos Toibero, Ricardo Carelli. Passivity based visual servoing of mobile robots with dynamics compensation. Mechatronics, 2012; 22 (4): 481-490.

[15] Jee-Hwan Ryu, Dong-Soo Kwon, and Blake Hannaford. Stable Teleoperation with Time-Domain Passivity Control. IEEE Trans. Robot. Automat., 2004; 20 (2): 365–373.

[16] Ran Tao and Mahdi Tavakoli. Multilateral Haptic System Stability Analysis: The Effect of Activity or Passivity of Terminations via a Series-Shunt Approach. In: Proceedings of the IEEE Haptics Symposium, Houston, 2014. p. 203-208.

[17] Weihua Li, Liang Ding, Haibo Gao et al. ROSTDyn: Rover simulation based on terramechanics and dynamics. J Terramech 2013; 50: 199-210.

[18] R. Lozano, B. Maschke, B. Brogliato, and O. Egeland, Dissipative Systems Analysis and Control: Theory and Applications. Secaucus, NJ, USA: Springer-Verlag New York, Inc., 2007.

[19] F. B. Llewellyn. Some fundamental properties of transmission systems. Proceedings of the IRE, 1952; 40 (3): 271–283.

[20] Mahdi Tavakoli, Arash Aziminejad, Rajni V. Patel, and Mehrdad Moallem. High-Fidelity Bilateral Teleoperation Systems and the Effect of Multimodal Haptics. IEEE Trans. Syst. Man Cybern.-Part B, 2007; 37 (6): 1512-1528.

[21] The Rover Team. Characterization of the Martian Surface Deposits by the Mars Pathfinder Rover, Sojourner. Science 1997; 278(5344): 1765-1768.

[22] MC Cavusoglu, D Feygin, F Tendick. A Critical Study of the Mechanical and Electrical Properties of the PHANToM Haptic Interface and Improvements for High Performance Control. Presence: Teleoperators & Virtual Environments 11 (6), 555-568.

[23] Haibo Gao, Weihua Li, Liang Ding et al. A Method for On-line Soil Parameters Modification to Planetary Rover Simulation. J Terramech 2012; 49: 325-339.

[24] Weihua Li, Zhen Liu, Haibo Gao, Liang Ding, Nan Li and Zongquan Deng. Soil Parameter Modification Used for Boosting Predictive Fidelity of Planetary Rover's Slippage. J. Terramech., 2014; 56: 173-184.